Int. Conference on Boundary and Interior Layers
BAIL 2006
G. Lube, G. Rapin (Eds)

Numerical Approximation of Flow Induced Airfoil Vibrations *

Petr Sváček

Department of Technical Mathematics, Karlovo náměstí 13,
121 35 Praha 2, CTU, Faculty of Mechanical Engineering.

1. Introduction

The research in aeroelasticity or hydroelasticity focuses on the interaction between moving fluids and vibrating structures (see, e.g. [3], [3] [6]). Widely used commercial codes, as e.g. NASTRAN, FLUENT or ANSYS, can solve only special problems of aeroelasticity or hydroelasticity and are mainly limited to linearized models. By NASTRAN the critical fluid flow velocity can be determined, but the post-flutter behaviour and other nonlinear phenomena for large amplitudes of vibration cannot be captured. Since the appearance of any aerodynamic instability is not admissible in normal flight regimes, the nonlinear postcritical limit states usually had not been considered. Recently, the modelling of post-flutter behaviour began to be more important.

In this paper we are interested in the interaction of two dimensional incompressible viscous laminar flow and a flexibly supported airfoil. The numerical simulation of such a problem is very challenging topic - it consists of discretization and stabilization of the Navier-Stokes equations for a high Reynolds number, the solution of the nonlinear and linear problems, the solution on time dependent computational domain, the numerical approximation of the structure model and the coupling algorithm.

In the paper we focus on the fluid flow approximation. The problem is discretized by the higher order finite element method(FEM). The Galerkin FEM leads to unphysical solutions if the grid is not fine enough in regions of strong gradients (e.g. boundary layer). In order to obtain physically admissible correct solutions it is necessary to apply suitable mesh refinement combined with a stabilization technique giving stable and accurate schemes. In our paper we present a special version of the GLS stabilization method for Navier-Stokes equations.

Further, the computation of the aerodynamical force acting on the airfoil requires correct evaluation of boundary integral of the stress tensor. A straightforward evaluation of the stress tensor integral may lead to inaccurate results. This obstacle is avoided with the aid of a weak formulation of the force acting on the profile.

2. Problem description

Mathematical model for the relevant technical application consists of fluid and airfoil models. First, the fluid flow is described with the aid of the incompressible Navier-Stokes system of equations written in Arbitrary Lagrangian-Eulerian (ALE) formulation, see, e.g., [7]. The ALE method combines the use of the classical Lagrangian and Eulerian reference frames (see, e.g. [4]).The fixed in space Eulerian reference frame is the typical framework used in the analysis of fluid mechanics problems. One of the disadvantages of the Eulerian system is that it does not track the path of any element, in particular the moving fluid-structure interface.

The Lagrangian reference frame is usually used in solid mechanics. It sets up the reference frame by fixing a grid to the material of interest. The material deformation causes also the grid deformation. On the other hand, the use of Lagrangian reference frame for fluid flow is

*This research was supported under grant No. 201/05/P142 of the Grant Agency of Czech Republic and under Research Plan MSM 6840770003 of the Ministry of Education of the Czech Republic.

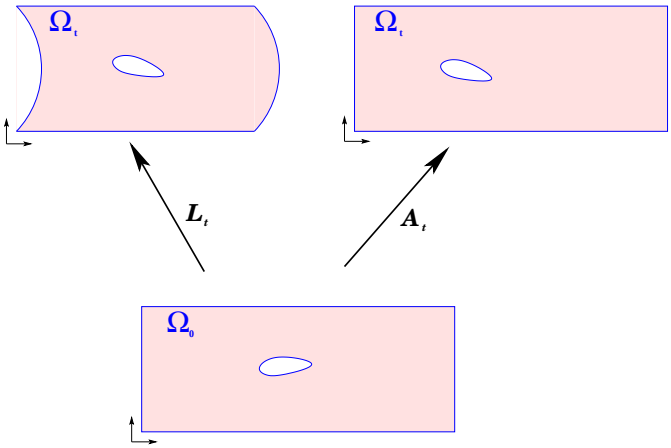

Figure 1: Comparison of Lagrangian and Arbitrary Lagrangian-Eulerian mappings.
In this figure the demonstration of Lagrangian mapping (on the left) and ALE mapping (on the right) is shown. Although the Lagrangian mapping allows the structure to be deflected, the other (artificial) boundaries are also deformed , which is unusable in practical computations. ALE mapping is then the "compromise" between having fixed artificial boundaries and deflected the structure boundary.

not suitable as the fluid particles travel independent of each other, which causes excessive grid deformations. In what follows we start by introducing the ALE mapping $\mathcal{A}_t$. The ALE mapping is a generalization of the Lagrangian mapping, which follows motion of all particles of the original domain Ω_0, i.e. the Lagrangian mapping is the mapping $\mathcal{L}_t : \Omega_0 \to \Omega_t$, such that $\mathcal{L}_t(\xi) \in \Omega_t$ is the position of the fluid partical at time t originally located at the position $\xi \in \Omega_0$. The comparison of Lagrangian and ALE mappings is shown in Figure 1.

The ALE mapping $\mathcal{A}_t$ maps the reference configuration Ω_0 onto the computational domain at time t Ω_t (i.e. the current configuration).

$$\begin{aligned} \mathcal{A}_t : \Omega_0 &\mapsto \Omega_t, \\ Y &\mapsto y(t, Y) = \mathcal{A}_t(Y). \end{aligned}$$

By the differentiating of ALE mapping $\mathcal{A}_t$ with respect to time, the **domain velocity** $\mathbf{w}_g$ is computed in the reference coordinates $\widetilde{\mathbf{w}}_g(t, Y) = \frac{\partial y}{\partial t}(t, Y)$ and transformed to spatial coordinates y as $\mathbf{w}_g(t, y)$. The time derivative with respect to the original configuration is then called **ALE derivative**, it is denoted as $\frac{D^{\mathcal{A}} f}{Dt}$ and can be computed as

$$\frac{D^{\mathcal{A}} f}{Dt} = \frac{\partial f}{\partial t} + (\mathbf{w}_g \cdot \nabla) f. \tag{1}$$

With the aid of the ALE derivative $\frac{D^{\mathcal{A}} f}{Dt}$ the Navier-Stokes system of equations can be rewritten as

$$\begin{aligned} \frac{D^{\mathcal{A}_t} \mathbf{u}}{Dt} - \nu \triangle \mathbf{u} + \Big((\mathbf{u} - \mathbf{w}_g) \cdot \nabla \Big) \mathbf{u} + \nabla p = 0, \qquad & \text{in } \Omega_t \times (0, T), \\ \nabla \cdot \mathbf{u} = 0, \qquad & \text{in } \Omega_t \times (0, T), \end{aligned} \tag{2}$$

where by Ω_t we denote the computational domain occupied by fluid at time t, $\mathbf{u}$ denotes the velocity vector, p - denotes the kinematic pressure (i.e. the dynamic pressure divided by the air density) and by $\mathbf{w}_g$ the domain velocity vector is denoted. On the boundary $\partial\Omega$ we prescribe suitable boundary conditions. First, the boundary $\partial\Omega$ is decomposed into three distinct parts, i.e. $\partial\Omega = \Gamma_{W_t} \cup \Gamma_D \cup \Gamma_O$. On Γ_D and Γ_{W_t} the Dirichlet boundary is prescribed, i.e.

$$\text{a)} \quad \mathbf{u} = \mathbf{u}_D \text{ on } \Gamma_D, \qquad \text{b)} \quad \mathbf{u} = \mathbf{w}_g \text{ on } \Gamma_{W_t}. \tag{3}$$

The latter part of boundary denoted by the symbol Γ_{W_t} is the only moving part of the boundary. The boundary Γ_O represents the outlet, where the *do-nothing* boundary condition is prescribed

$$\Big[-(p-p_{ref})\mathbf{n}+\nu\frac{\partial \mathbf{u}}{\partial \mathbf{n}}\Big]\Big|_{\Gamma_O}=0, \tag{4}$$

The weak formulation of the equation (2) then can be introduced: Find a velocity vector $\mathbf{u}\in \big(H^1(\Omega_t)\big)^2$ with Dirichlet boundary conditions (3) satisfied and a pressure $p\in L^2(\Omega_t)$, such that for all test functions $\mathbf{v}\in X\subset \big(H^1(\Omega_t)\big)^2$ (being zero on Dirichlet part of boundary) and for all pressure test functions $q\in Y=L^2(\Omega_t)$ the following equation is holds

$$\begin{aligned}\Big(\frac{D^{\mathcal{A}}\mathbf{u}}{Dt},\mathbf{v}\Big)+\nu((\mathbf{u},\mathbf{v}))+\mathbf{c}(\mathbf{u};\mathbf{u},\mathbf{v})-\Big((\mathbf{w}_g\cdot\nabla)\mathbf{u},\mathbf{v}\Big)\\ -\Big(p,\nabla\cdot\mathbf{v}\Big)+\Big(\nabla\cdot\mathbf{u},q\Big)+\int_{\Gamma_O}\frac{1}{2}(\mathbf{u}\cdot\mathbf{n})^{+}\mathbf{u}\cdot\mathbf{v}dS &= 0\end{aligned} \tag{5}$$

where

$$\begin{aligned}\mathbf{c}(\mathbf{b};\mathbf{u},\mathbf{v}) &= \int_{\Omega_t}\left(\frac{1}{2}(\mathbf{b}\cdot\nabla)\,\mathbf{u}\cdot\mathbf{v}-\frac{1}{2}(\mathbf{b}\cdot\nabla)\,\mathbf{v}\cdot\mathbf{u}\right)dx,\\ ((\mathbf{u},\mathbf{v})) &= \int_{\Omega_t}(\nabla\mathbf{u})\cdot(\nabla\mathbf{v})dx,\end{aligned} \tag{6}$$

and by $\Big(\cdot,\cdot\Big)$ the scalar product on $L^2(\Omega_t)$ or $\big(L^2(\Omega_t)\big)^2$ is denoted.

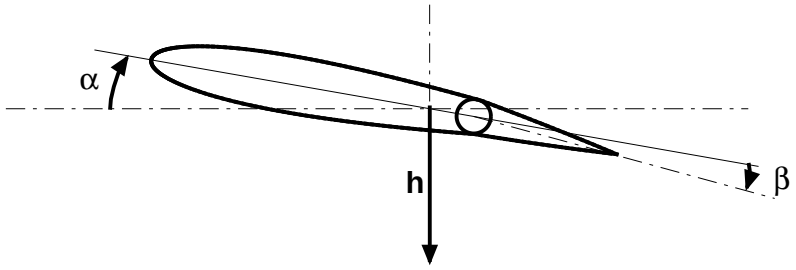

Figure 2: Airfoil pitching, plunging and rotation of the flap

2..1. STRUCTURE MODEL

A typical section airfoil (semichord b) in subsonic air flow is considered as shown in Figure 2. A trailing edge flap is hinged at $c_\beta\, b$ after the midchord. By h, α and β the plunging of the elastic axis, pitching of the airfoil and rotation of the flap is denoted, respectively (see Figure 3). The system motion generates unsteady aerodynamic lift $L=L(t)$, aerodynamic moment $M=M(t)$ and hinge moment $M_\beta=M_\beta(t)$. By k_h, k_α and k_β the spring constant of wing bending, wing torsional stiffness and flap hinge moment are denoted, respectively. The mass matrix is defined by the mass m and the moment of inertia I_α of the entire airfoil around the elastic axis. The flap moment of inertia around the hinge is denoted by I_β. The equations of motion for a flexibly supported rigid airfoil, read

$$\mathbb{M}\,\ddot{\mathbf{u}}+\mathbb{B}\dot{\mathbf{u}}+\mathbb{K}\,\mathbf{u}+\mathbf{f}_{NL}(\mathbf{u})=\mathbf{f}, \tag{7}$$

where

$$\mathbb{M} = \begin{pmatrix} m & S_\alpha & S_\beta \\ S_\alpha & I_\alpha & (c_\beta - e)bS_\beta + I_\alpha \\ S_\beta & (c_\beta - e)bS_\beta + I_\alpha & I_\beta \end{pmatrix}, \quad \mathbb{K} = \begin{pmatrix} k_h & 0 & 0 \\ 0 & k_\alpha & 0 \\ 0 & 0 & k_\beta \end{pmatrix},$$

$$\mathbb{D} = \begin{pmatrix} d_h & 0 & 0 \\ 0 & d_\alpha & 0 \\ 0 & 0 & d_\beta \end{pmatrix},$$

and $\mathbf{u} = (h, \alpha, \beta)^T$, $\mathbf{f} = (-L, M, M_\beta)^T$. By $\mathbf{f}_{NL}$ the nonlinear terms are denoted.

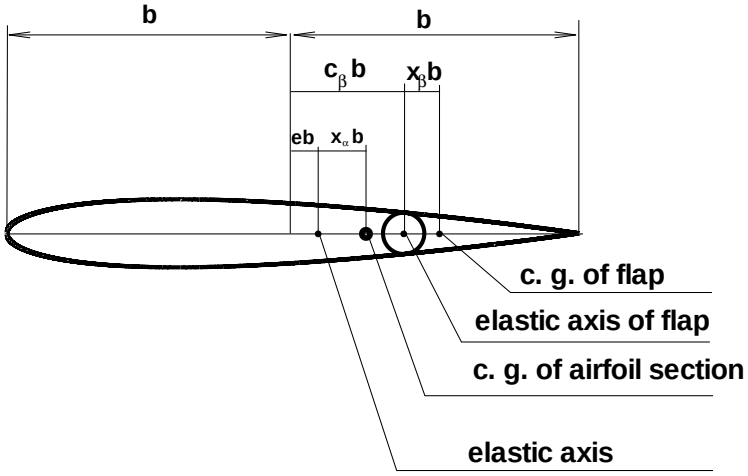

Figure 3: Typical airfoil section with three degrees of freedom.
By b the semichord of the airfoil is denoted, $e\,b$ denotes the location of the elastic axis of the wing after midchord, $x_\alpha\,b$ the location of the center of gravity after the elastic axis, $c_\beta\,b$ denotes the location of the flap hinge after the midchord and $x_\beta\,b$ the location of the center of gravity of the flap.

3. Time discretization

First, let start with the equidistant discretization of the time interval $[0, T]$ with the time step Δt, i.e. $t_k = k \cdot \Delta t$ for $k = 0, 1, 2, \ldots$. Let $\mathbf{u}_n, p_n$ denote the approximation of velocity vector $\mathbf{u}$ and pressure p evaluated at the time level t_n, i.e. $\mathbf{u}_n \approx \mathbf{u}(t_n)$ and $p_n \approx p(t_n)$. The ALE derivative of the velocity vector $\mathbf{u}$ then is approximated as

$$\frac{D^{\mathcal{A}_t} f}{Dt} \approx \frac{3\mathbf{u}_{n+1} - 4\hat{\mathbf{u}}_n + \hat{\mathbf{u}}_{n-1}}{2\Delta t}, \tag{8}$$

where the velocity $\mathbf{u}_{n+1}$ denotes the approximate velocity at time t_{n+1} and the velocities $\hat{\mathbf{u}}_n, \hat{\mathbf{u}}_{n-1}$ are the velocities at previous time steps t_n and t_{n-1} transformed from domains $\Omega_{t_n}, \Omega_{t_{n-1}}$ on the current computational domain $\Omega_{t_{n+1}}$, i.e., $\hat{\mathbf{u}}_n \equiv \mathbf{u}_n \circ \mathcal{A}_{t_n} \circ \mathcal{A}_{t_{n+1}}^{-1}$, $\hat{\mathbf{u}}_{n-1} \equiv \mathbf{u}_{n-1} \circ \mathcal{A}_{t_{n-1}} \circ \mathcal{A}_{t_{n+1}}^{-1}$.

4. Space discretization

The approximate solution of the time discretized problem (5), (8) will be sought in the space of the triangular conforming piecewise polynomial elements. For the sake of clarity, we restrict ourselves on the time moment $t = t_{n+1}$ and we denote the computational domain $\Omega = \Omega_{t_{n+1}}$.

Furthermore, we will use a triangulation τ_Δ of the domain Ω_t and on every element $K \in \tau_\Delta$ the local element spaces P_K and Q_K for velocity components and pressure are defined. The construction of the base functions is based on the local element polynomial degree. In order to guarantee continuity of the base functions, the minimum rule has to be applied, see, e.g., [8].

The space X_Δ of fluid velocity vectors is then introduced

$$X_\Delta = H^2_\Delta, \qquad H_\Delta = \{v \in C(\overline{\Omega}); v|_K \in P_K \subset P_k(K) \text{ for each } K \in \tau_\Delta\},$$

and the pressure space Y_Δ defined as

$$Y_\Delta = \{v \in C(\overline{\Omega}); v|_K \in Q_K \subset P_k(K) \text{ for each } K \in \tau_\Delta\}.$$

Moreover, we define the space of test functions being zero on the Dirichlet part of boundary

$$X_{\Delta,0} = \{\mathbf{v} \in X_\Delta \ : \ \mathbf{v}|_{\Gamma_D \cup \Gamma_{W_{t_{n+1}}}} = 0\}.$$

The standard Galerkin approximation of the weak formulation (5) may suffer from two sources of instabilities. One instability is caused by a possible incompatibility of pressure and velocity pairs. It can be overcome either by the use of the finite element velocity/pressure pair, that satisfy the Babuška-Breezi condition, or by the use of pressure stabilizing terms. Further, the dominating convection requires to introduce some stabilization of the finite element scheme, as, e.g. upwinding or streamline-diffusion method. In order to overcome both difficulties, the Galerkin Least Squares method can be applied, see, e.g. ([5]). First, we start with definition of standard Galerkin terms, SUPG/GLS stabilizing term and grad-div stabilizing terms, for details see [5], [9].

The Galerkin terms are defined as

$$\begin{aligned} \mathbf{a}(\mathbf{u}^*; U_\Delta, V_\Delta) &= \frac{3}{2\Delta t}(\mathbf{u}, \mathbf{v})_\Omega + \nu(\nabla \mathbf{u}, \nabla \mathbf{v})_\Omega + \mathbf{c}(\mathbf{u}^*; \mathbf{u}, \mathbf{v}) \\ &\quad - \left((\mathbf{w}_g^{n+1} \cdot \nabla)\,\mathbf{u}, \mathbf{v}\right)_\Omega - (p, \nabla \cdot \mathbf{v})_\Omega + (\nabla \cdot \mathbf{u}, q)_\Omega\,, \\ f(\mathbf{u}, \mathbf{v}) &= \frac{1}{2\Delta t}(4\hat{\mathbf{u}}_n - \hat{\mathbf{u}}_{n-1}, \mathbf{v})_\Omega - \int_{\Gamma_O} p_{\text{ref}}(\mathbf{v} \cdot \mathbf{n})\, dS. \end{aligned} \tag{9}$$

Next, we define the SUPG/GLS stabilizing terms

$$\begin{aligned} \mathcal{L}(\mathbf{u}^*; U_\Delta, V_\Delta) &= \sum_{K \in T_\Delta} \delta_K \Big(\frac{3}{2\Delta t}\mathbf{u} - \nu \triangle \mathbf{u} + ((\mathbf{u}^* - \mathbf{w}_g) \cdot \nabla)\,\mathbf{u} + \nabla p, \psi(\mathbf{u}^*, q) \Big)_K, \\ \mathcal{F}(V_\Delta) &= \sum_{K \in T_\Delta} \delta_K \Big(\frac{1}{2\Delta t}(4\hat{\mathbf{u}}_n - \hat{\mathbf{u}}_{n-1}), \psi(\mathbf{u}^*, q) \Big)_K, \end{aligned} \tag{10}$$

where $\psi(\mathbf{u}^*, q) \equiv ((\mathbf{u}^* - \mathbf{w}_g) \cdot \nabla)\,\mathbf{v} + \nabla q$. The grad-div stabilizing terms $\mathcal{P}(U_\Delta, V_\Delta)$ are defined as

$$\mathcal{P}(U_\Delta, V_\Delta) = \sum_{K \in T_\Delta} \tau_K (\nabla \cdot \mathbf{u}, \nabla \cdot \mathbf{v})_K, \tag{11}$$

The stabilized discret problem: *Find $U_\Delta = (\mathbf{u}, p) \in H_\Delta \times Y_\Delta$ such that $\mathbf{u}$ satisfies approximately the Dirichlet boundary conditions (3) and the equation*

$$\mathbf{a}(\mathbf{u}; U_\Delta, V_\Delta) + \mathcal{L}(\mathbf{u}; U_\Delta, V_\Delta) + \mathcal{P}(U_\Delta, V_\Delta) = f(V_\Delta) + \mathcal{F}(V_\Delta), \tag{12}$$

holds for all $V_\Delta = (\mathbf{v}, q) \in X_{\Delta,0} \times Y_\Delta$.

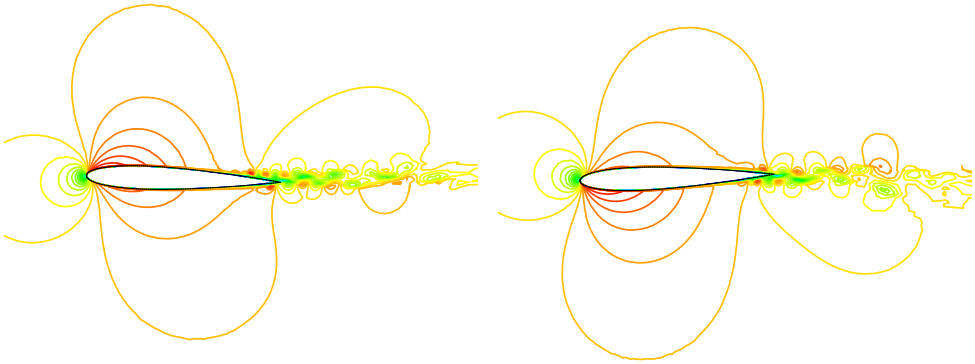

Figure 4: The velocity distribution around the airfoil NACA 0012 for the angle of attack varying in time

The choice of the parameters δ_K and τ_K depends on the chosen pair of local elements P_K/Q_K. Here, we distinguish between the Taylor-Hood family of finite element pairs and all the other finite element pairs.

In the case of the local element pair P_K, Q_K being of the Taylor-Hood family P^{m+1}/P^m the following choice of parameters is used

$$\tau_K = \tau_*, \qquad \delta_K = \delta^* h^2,$$

where $\tau^* > 0$ and $\delta^* > 0$ are fixed constants (e.g., we usually set $\tau^* = \delta^* = 1$). The local element size h depends on the local element, local stream velocity vector and the local element degree deg P_K of the velocity approximation.

In the case when the local element pair P_K/Q_K does not belong to the Taylor-Hood family $P^{m+1}(K)/P^m(K)$, the following choice of parameters is used

$$\tau_K = \nu \cdot \left(1 + Re^{loc} + \frac{h^2}{\nu \cdot \Delta t}\right), \qquad \delta_K = \frac{h^2}{\tau_K},$$

where the local Reynolds number is defined as $Re^{loc} = \frac{h\|\mathbf{u}\|_K}{2\nu}$.

5. Numerical solution

In order to find the solution of the nonlinear problem (12) coupled with (7), the strong coupling algorithm will be used on every time level t_{n+1}

- First, using the extrapolation of aerodynamical forces the system of ODE (7) is used, and the approximate computational domain $\Omega \approx \Omega_{t_{n+1}}$ is determined.
- Next, the problem (12) is solved on the domain $\Omega \approx \Omega_{t_{n+1}}$ using Oseen linearization.
- Using the approximate velocity $\mathbf{u}_{n+1}$ and pressure p_{n+1} the aerodynamical forces are updated. We continue with the first step until the convergence is obtained.

The system of ODEs (7) on time interval $[t_k, t_{k+1}]$ is solved by fourth order Runge-Kutta method, where the approximate values α_k and h_k are used instead of the exact ones $\alpha(t_k)$ and $h(t_k)$. The values of α_k and h_k determines the transformation of domain $\Omega_k \equiv \Omega_{t_k}$. In order to proceed from time level t_k to the time level t_{k+1} the approximate value of the aerodynamical lift force $\tilde{L} \approx L(t_{k+1})$ and the approximate value of the aerodynamical torsional moment $\tilde{M} \approx M(t_{k+1})$ are employed.

The solution of the nonlinear problem (12) is performed by Oseen linearizations, i.e. we start from approximation $U_\Delta^{(0)} = (\mathbf{u}^{(0)}, p^{(0)})$, and for $i = 0, \ldots, N_n - 1$ we solve the problem find $U_\Delta^{(i+1)} = (\mathbf{u}^{(i+1)}, p^{(i+1)})$

$$\mathbf{a}(\mathbf{u}^{(i)}, {U_\Delta}^{(i+1)}, V_\Delta) + \mathcal{L}({U_\Delta}^{(i)}, {U_\Delta}^{(i+1)}, V_\Delta) + \mathcal{P}({U_\Delta}^{(i+1)}, V_\Delta) = f(V_\Delta) + \mathcal{F}(V_\Delta),$$

then set the solution of the nonlinear problem $U_\Delta = U_\Delta^{(N_n)}$. In practical computation it is enough to compute 3-10 iterations.

5..1. Numerical results

The numerical simulation of flow over NACA 0012 airfoil, whose vibrations is either given analytically or obtain by the solution of the system of ODEs (7), are presented in Figures 5-7. In the first case, the numerical approximations of the airfoil surface values of the pressure coefficient

$$c_p = \frac{p - p_0}{\frac{1}{2}\rho U^2}$$

was compared with the experimental data from [1]. The time dependence of the rotational angle of the airfoil was prescribed as the periodical function with the frequency 30 Hz and the amplitude 3 degrees, the far field velocity is $U_\infty = 136\ \mathrm{m\,s^{-1}}$ and the length of airfoil chord is $L = 0.1322$ m (see Figure 5).

Furthermore, the simulation of the coupled model (5) and (7) in the case of 2 degrees of freedom is presented in the case of the flexibly supported airfoil NACA 0012 in Figures 6-7. The solution was performed for far field velocities $U_\infty = 5\mathrm{m\,s^{-1}}$, $U_\infty = 26\mathrm{m\,s^{-1}}$ and the choice of parameter's values from report [2] was used.

References

[1] J. Benetka and J. Horáček. Experimental pressure data on vibrating airfoils NACA 64A012M5 and NACA 0012. Technical report, Institute of Thermomechanics, Czech Academy of Sciences, 2003.

[2] J. Čečrdle and J. Maleček. Verification FEM model of an aircraft construction with two and three degrees of freedom. Technical Report Research Report R-3418/02, Aeronautical Research and Test Institute, Prague, Letňany, 2002.

[3] E. H. Dowell. *A Modern Course in Aeroelasticity.* Kluwer Academic Publishers, Dodrecht, 1995.

[4] M. Feistauer. *Mathematical Methods in Fluid Dynamics.* Longman Scientific & Technical, Harlow, 1993.

[5] T. Gelhard, G. Lube, and M. A. Olshanskii. Stabilized finite element schemes with LBB-stable elements for incompressible flows. *Journal of Computational Mathematics*, 177:243–267, 2005.

[6] E. Naudasher and D. Rockwell. *Flow-Induced Vibrations.* A.A. Balkema, Rotterdam, 1994.

[7] T. Nomura and T. J. R. Hughes. An arbitrary Lagrangian-Eulerian finite element method for interaction of fluid and a rigid body. *Computer Methods in Applied Mechanics and Engineering*, 95:115–138, 1992.

[8] P. Solin, K. Segeth, and I. Dolezel. *Higher-Order Finite Element Methods.* Chapman & Hall/CRC Press, 2003.

[9] Sváček, P. , M. Feistauer, and J. Horáček. Numerical simulation of flow induced airfoil vibrations with large amplitudes. *Journal of Fluids and Structures*, 2004. (submitted).

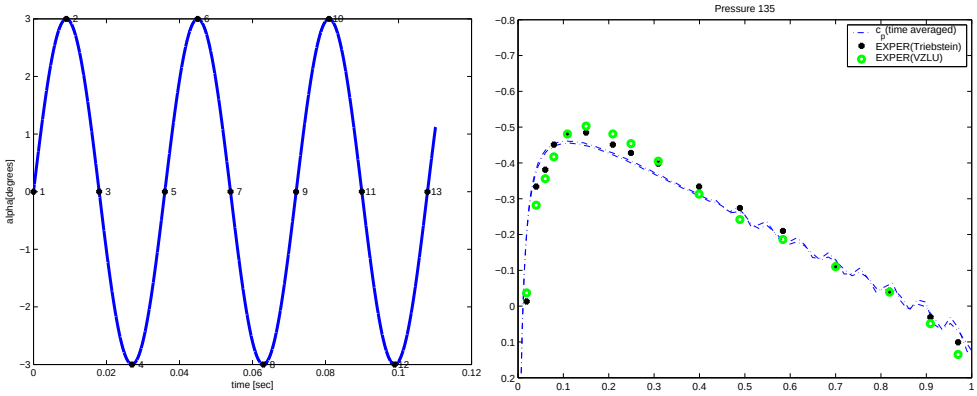

Figure 5: Dependence of α on time t for vibrating airfoil with frequency 30 Hz and amplitude 3 degrees (on the left). On the right the comparison of the time averaged coefficient c_p along the profile NACA 0012 with the experimental data.

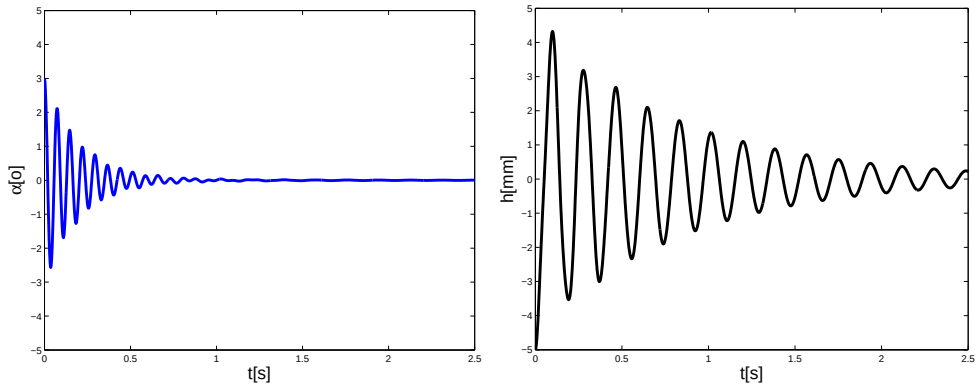

Figure 6: The damped vibrations in h and α of flexibly supported airfoil NACA 0012 for far field velocity $U_\infty = 5\,\mathrm{m\,s}^{-1}$.

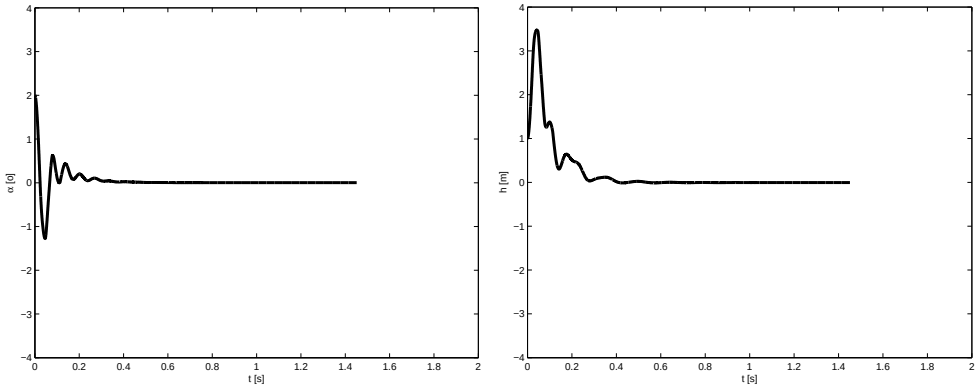

Figure 7: The damped vibrations in h and α of flexibly supported airfoil NACA 0012 for far field velocity $U_\infty = 26\,\mathrm{m\,s}^{-1}$.